DOI: 10.1002/adma.200602437

Ultrafast Electron Transfer and Decay Dynamics in a Small Band Gap Bulk Heterojunction Material**

By *In-Wook Hwang*, *Cesare Soci*, *Daniel Moses*,* *Zhengguo Zhu*, *David Waller*, *Russell Gaudiana*, *Christoph J. Brabec*, and *Alan J. Heeger**

Bulk heterojunction materials comprising bicontinuous networks of electron donor and acceptor components sandwiched between electrodes with different work functions (e.g., indium-tin oxide, ITO, and a lower work-function metal such as Al) have yielded the best results to date for organic polymer-based solar cells. In such bulk heterojunction materials, ultrafast photoinduced electron transfer occurs at the interface between the polymer (donor) and the fullerene (acceptor) and results in efficient charge separation. Provided that the back transfer rate is sufficiently slow, the photo-generated mobile positive and negative carriers can be collected at the electrodes; electrons at the lower work function electrode and holes at the higher work function electrode.

Using this approach, power conversion efficiencies of 5 % have been demonstrated in bulk heterojunction materials comprised of poly(3-hexylthiophene), P3HT and the [6,6]-phenyl-C_{61} butyric acid methyl ester fullerene derivative, PCBM.[1,2] Although the quantum efficiency is high within the absorption spectrum, the band gap of this conjugated polymer is too large (the solar radiation spectrum extends into the infrared). Thus, the quest for higher solar cell efficiencies has focused on smaller band gap polymers designed and synthesized to improve the harvesting of solar radiation.[3–10]

Here we describe the results of time-resolved spectroscopic studies of the small band gap semiconducting copolymer, poly[2,6-(4,4-bis-(2-ethylhexyl)-4*H*-cyclopenta[2,1-*b*;3,4-*b*′]dithiophene)-*alt*-4,7-(2,1,3-benzothiadiazole)], PCPDTBT, made of alternating electron-rich and electron-deficient units and in bulk heterojunction materials comprising PCPDTBT and PCBM. The molecular structures of PCPDTBT and PCBM are shown in Scheme 1. Because carrier recombination prior to collection at the electrodes would limit the photovoltaic power conversion efficiency, the goal of our studies was to demonstrate ultrafast photoinduced electron transfer and to study the carrier recombination dynamics following photo excitation.

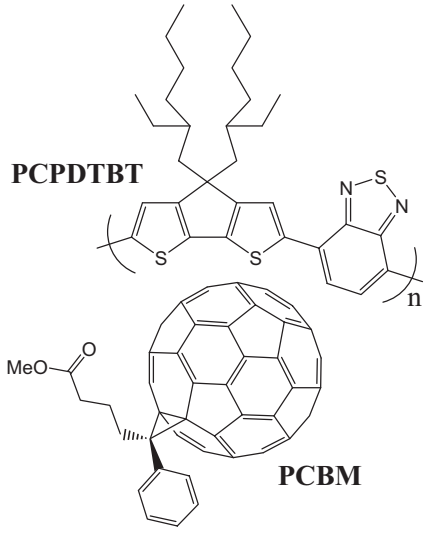

Scheme 1. Molecular structures of PCPDTBT and of PCBM; the molecular weight of PCPDTBT used was approximately 30 000 g mol^{-1}.

As in most bulk heterojunction materials made from mixtures of conjugated polymers with C_{60} and its derivatives (e.g., poly(*p*-phenylene vinylene)s:C_{60}[11–15] and poly(thiophene)s:C_{60}[12,16,17]), we find that in PCPDTBT:PCBM, photo excitation initiates ultrafast (sub-picosecond) electron transfer from the polymer to the PCBM. This electron transfer reaction is faster by two orders of magnitude than the singlet-state lifetime in the pristine polymer. From analysis of the carrier recombination dynamics, we infer the existence of an intermediate charge transferred state (possibly a bound state of an electron on the PCBM and a hole on a nearby PCPDTBT) from which long-lived mobile positive and negative carriers are subsequently generated; see Scheme 2. The yield of long-lived mobile carriers in PCPDTBT:PCBM composites is sensitive to the ratio of the components. The time-decay measurements indicate that the 1:3.3 composites exhibit the highest yield of long-lived mobile carriers, consistent with the obser-

[*] Dr. D. Moses, Prof. A. J. Heeger, Dr. I.-W. Hwang, Dr. C. Soci
Center for Polymers and Organic Solids
University of California Santa Barbara
Santa Barbara, CA 93106-5090 (USA)
E-mail: moses@physics.ucsb.edu; ajhe@physics.ucsb.edu
Z. Zhu, D. Waller, R. Gaudiana
Konarka Technologies, Inc.
116 John Street, Lowell, MA 01852 (USA)
Dr. C. J. Brabec
Konarka Technologies Austria
Altenbergerstrasse 69, 4040 Linz (Austria)

[**] We thank Dr. Jin Young Kim for making the high quality films used in this study. Research at UCSB was funded by a grant from National Science Foundation (NSF-DMR 0602280), support from Konarka Technologies, and from Korea Research Foundation (KRF-2005-M01-2004-000-20037-0-C00179).

ADVANCED MATERIALS

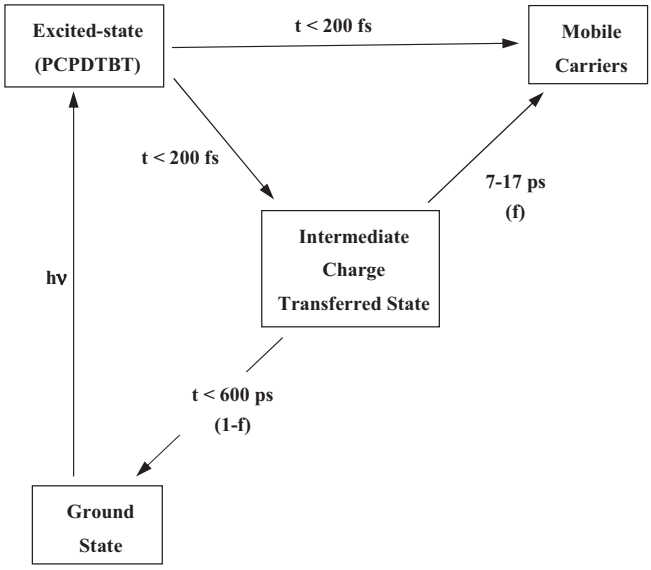

Scheme 2. In the annealed 1:3.3 PCPDTBT:PCBM composite, the intermediate charge transferred state converts almost completely (in $t < 7$ ps) to long-lived mobile carriers. In the 1:1 PCPDTBT:PCBM composites, there is only partial conversion ($f < 1$) to mobile carriers. The fraction $(1-f)$ decays to the ground state in $t < 600$ ps.

vation that the best solar cell efficiency is obtained using the 1:3.3 PCPDTBT:PCBM bulk heterojunction material after annealing at 120 °C for 10 minutes.

Figure 1 shows the steady-state absorption spectra of films of pristine PCPDTBT and the PCPDTBT:PCBM composites. PCPDTBT films absorb light over a wide spectral range, from the ultraviolet to ~900 nm (absorption edge of 1.46 eV, $\lambda \sim 850$ nm). The absorption peak from a pristine PCPDTBT film at $\lambda \sim 775$ nm is red-shifted by approximately 70 nm from that of the polymer in solution in ortho-dichlorobenzene (not shown) implying increased interchain interaction and planarization/extension of the conjugated segments in the solid state. The absorption spectra of the PCPDTBT:PCBM composites are superpositions of the contributions of the two components (although the 1:1 composite exhibits a small blue shift with respect to the maximum absorption by films of pristine PCPDTBT). Figure 1 shows that the spectrum obtained from the annealed 1:3.3 composite exhibits a negligible blue shift compared to that found in the 1:1 composites, a result that may imply better interchain interaction and planarization/extension of the conjugated polymer segments in the annealed 1:3.3 composite.

The photoluminescence (PL) spectrum obtained from a film of PCPDTBT is shown in the inset of Figure 1. The PL intensity is quite low compared to that from emissive polymers such as poly(*p*-phenylene vinylene) and its soluble derivatives, a result that may indicate a dipole-forbidden ^1A_g state as the lowest excited state, similar to that observed in P3HT.[18] Incorporating PCBM (50 % by weight) into the PCPDTBT results in total quenching of the PL intensity. Energy transfer mechanisms can be ruled out as the source of the PL quenching because the band gap of PCPDTBT (1.46 eV) is smaller than that of PCBM (1.76 eV). Moreover, the enhanced photoconductivity[19] observed in PCPDTBT:PCBM is indicative of enhanced photoinduced charge carrier generation. The PL quenching and enhanced photoconductivity imply efficient electron transfer and charge separation in the PCPDTBT:PCBM bulk heterojunction material.

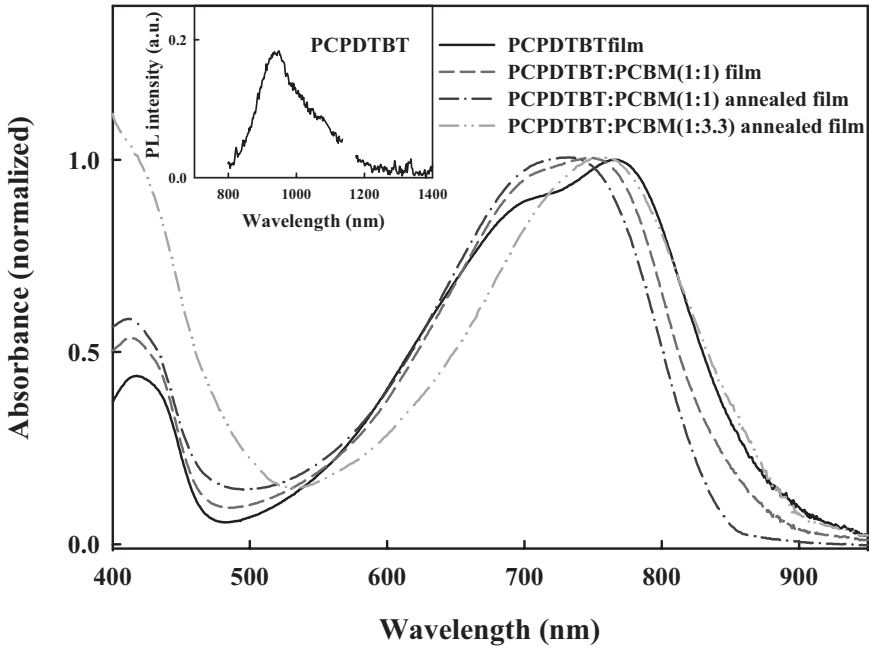

Figure 1. Steady-state absorption spectra obtained from films of PCPDTBT and PCPDTBT:PCBM bulk heterojunction materials (1:1 composites measured before and after annealing, and the 1:3.3 composite measured after annealing); the inset shows the photoluminescence spectrum of a PCPDTBT film measured before annealing when excited at 750 nm.

The transient absorption (TA) spectra for pristine PCPDTBT and for the PCPDTBT:PCBM composites, shown in Figure 2, demonstrate a clear difference in the spectral shape even at times as early time as 0.5 ps following photo excitation, indicative of ultrafast photoinduced electron transfer.

The spectrum for PCPDTBT (top panel) exhibits a photo-bleaching band centered at ~800 nm, matched with the steady-state absorption peak, and two photoinduced absorption (PIA) bands at 500–600 nm and in the infrared beyond 1100 nm. Note that all the TA bands from pristine PCPDTBT decay with a time constant of less than 100 ps.

The TA spectra of PCPDTBT:PCBM composites (the second, third, and fourth panels in Fig. 2) are significantly

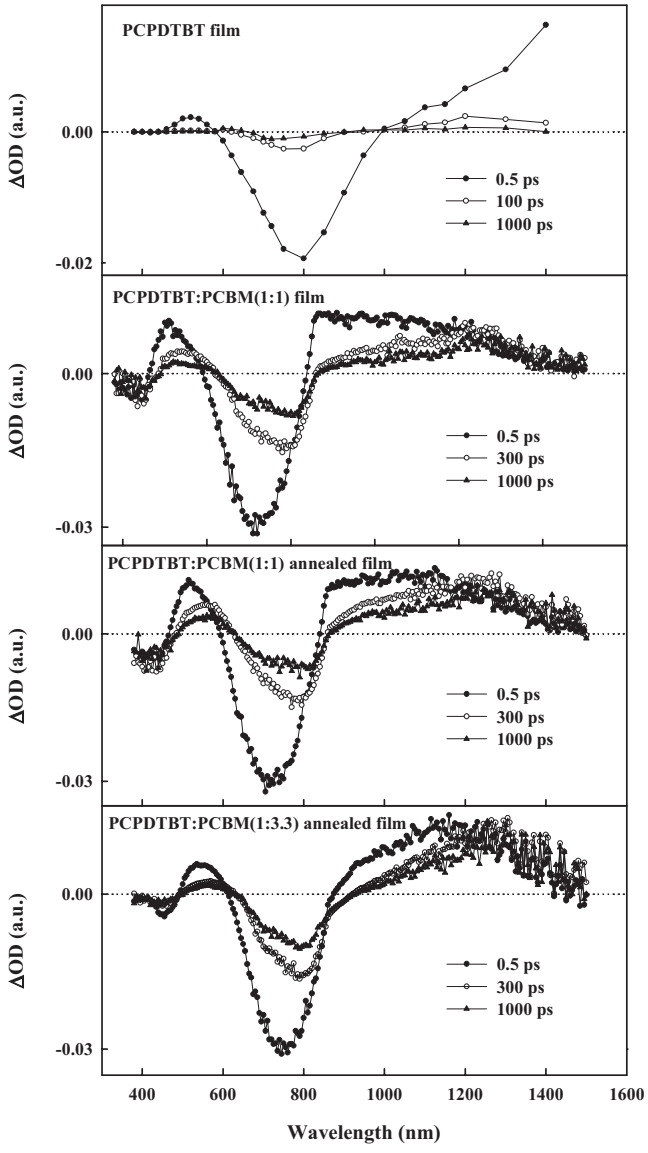

Figure 2. Transient absorption spectra obtained from films of PCPDTBT and PCPDTBT:PCBM bulk heterojunction materials (1:1 composites measured before and after annealing, and the 1:3.3 composite measured after annealing) at several delay times; the pump wavelength was 700 nm and intensity was 200 μJ cm^{-2}.

different from that of pristine PCPDTBT even at times as short as 0.5 ps following photo excitation: In particular, a new PIA band at ~900 nm appears within 0.5 ps after excitation and decays within 300 ps, while a longer-lived PIA centered at approximately 1200 nm persists with essentially constant amplitude for times beyond 1000 ps. These PIA bands, characteristic of PCPDTBT:PCBM composites, are ascribed to the two charge transferred states shown schematically in Scheme 2. Note the spectrum obtained from the annealed 1:3.3 composite, where the short-lived PIA band at ~900 nm is significantly reduced in magnitude compared to the same band found in the other composites. This reduced PIA at 900 nm is correlated with the higher solar cell efficiency obtained from annealed devices made with the 1:3.3 composite.

In Figure 2, one also sees that the peak of the photo-bleaching band in the PCPDTBT:PCBM composites is initially blue-shifted with respect to the bleaching in pristine PCPDTBT, but shifts at later times (after approximately 300 ps) to 800 nm;, i.e., the bleaching spectrum initially decays toward that of pristine PCPDTBT. The blue shift observed immediately after photo excitation implies an interaction between the hole on the PCPDTBT and an electron on a nearby PCBM during the time decay of the PIA at 900 nm. After the decay of the 900 nm PIA, the bleaching spectrum is essentially identical to that of pristine PCPDTBT indicating that the holes on the PCPDTBT network are well separated from the electrons on the PCBM network. At long times (>1000 ps), the 800 nm bleaching persists along with the 1200 nm PIA.

A more complete picture of ultrafast electron transfer in the PCPDTBT:PCBM composites is obtained from measurements of the PIA signals at earlier times (see Fig. 3). The PIA signals probed at ~900 nm rise within the experimentally determined 200 fs temporal resolution, implying that the dissociation of the singlet exciton in the polymer and the build-up of the initial charge transferred state occur at t < 200 fs for all PCPDTBT:PCBM ratios.

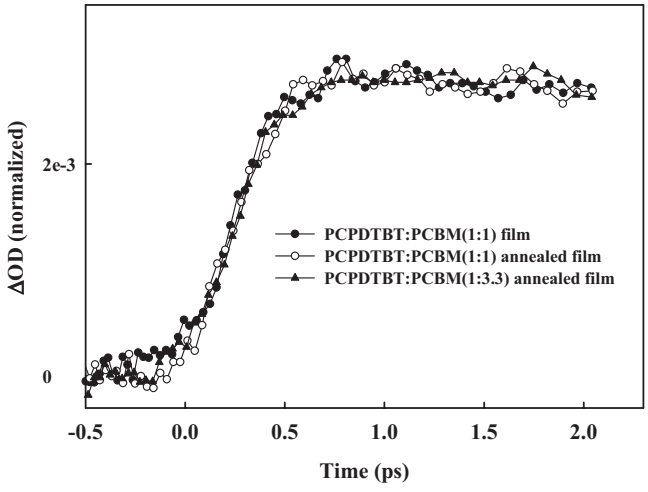

Figure 3. Ultrafast transient absorption signals obtained from PCPDTBT:PCBM films pumped at 700 nm and probed at 860 nm for the 1:1 composites measured before and after annealing, and at 920 nm for the 1:3.3 composite measured after annealing. For comparison, the data were normalized to the maximum values. The pump intensity was 40 μJ cm^{-2}; i.e., in the low intensity regime where the pump intensity did not affect the signal temporal profile.

The PIA decay profiles in pristine PCPDTBT are shown in the top panel of Figure 4. When probed at 1400 nm, the PIA-decay is well described by a bi-exponential term with time constants of 20 ps (61 %) and 120 ps (39 %). When probed at 1200 nm, similar initial time decay constants are observed

ADVANCED MATERIALS

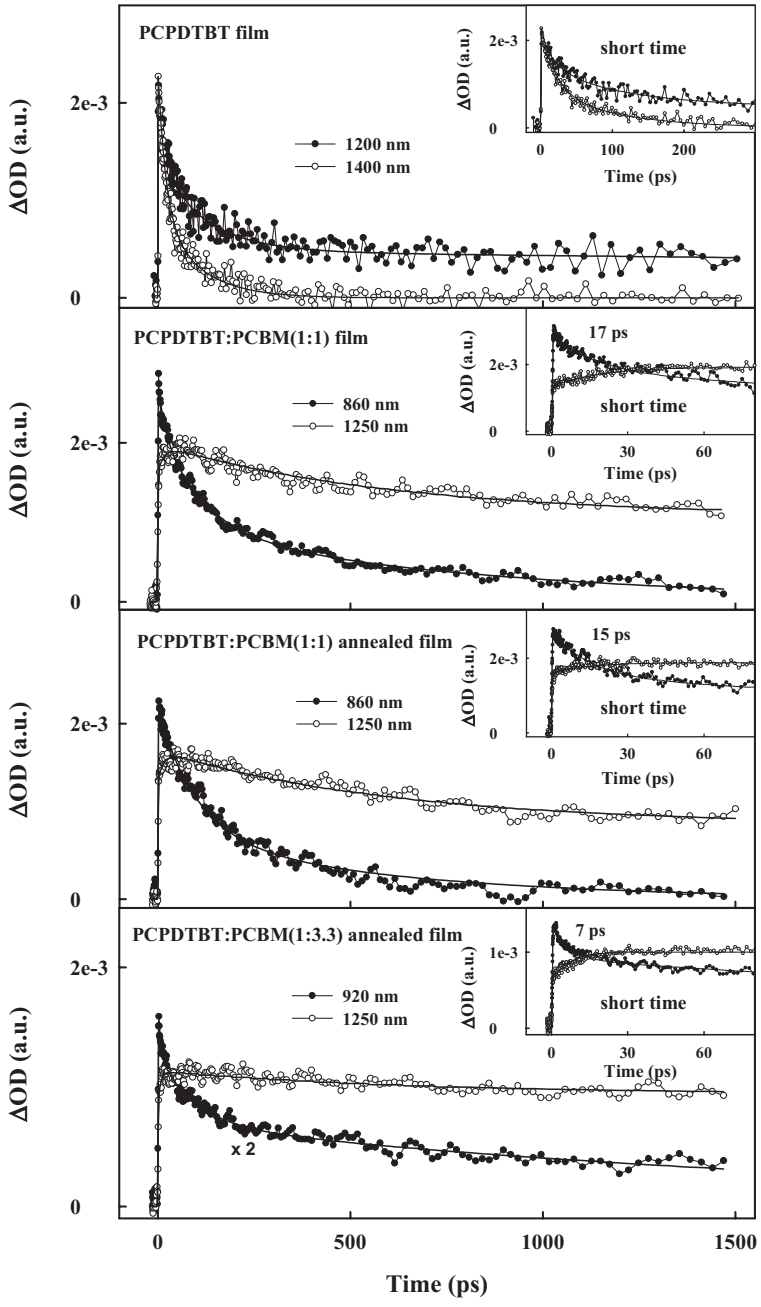

Figure 4. Transient absorption decay profiles obtained from films of PCPDTBT and PCPDTBT:PCBM bulk heterojunction materials (1:1 composites measured before and after annealing, and the 1:3.3 composite measured after annealing) probed at the wavelengths indicated in each panel; the pump wavelength was 700 nm and intensity was 40 μJ cm^{-2}; i.e., in the low intensity regime where the pump intensity did not affect the signal temporal profile. The insets of each panel reveal the decay profiles monitored with a higher temporal resolution.

(22 ps and 120 ps) followed by a residual signal which persists well beyond 1.5 ns. A weight averaging of the 20 ps and 120 ps contributions to the bi-exponential decay found at 1400 nm yields 60 ps as the approximate singlet-state lifetime in the pristine PCPDTBT film. This relatively short lifetime of the singlet excitons is similar to that observed in P3HT.[18,20,21] The longer-lived PIA at 1200 nm may arise from absorption by the photo excited carriers observed in the photoconductivity measurements of pristine PCPDTBT.

The data obtained from the PCPDTBT:PCBM composites (the second, third, and fourth panels in Fig. 4) generally show longer-lived PIA response, implying slower charge recombination dynamics. Note that the PIA-decay profile obtained from the composites is sensitive to both the probe wavelength and the ratio of PCPDTBT to PCBM. When probed at 1250 nm, all the composites exhibit a PIA component that is almost constant in the nanosecond time regime. There is, in addition, a component with a decay time constant of 500–600 ps, the magnitude of which is dependent on the PCPDTBT to PCBM ratio. For the 1:3.3 (annealed) material (fourth panel), the amplitude of the faster component is significantly reduced (nearly to zero) relative to that in the second and third panels. When probed at 860 or 920 nm, an initial PIA component characterized by a time constant of 200–300 ps is followed by long-lived PIA. At 860 or 920 nm, the long-lived PIA is much weaker than when probed at 1250 nm, consistent with the spectrum of the PIA bands shown in Figure 2.

The PIA signals in the picosecond time regime are shown with higher temporal resolution in the inset of each panel in Figure 4. The fast time decay (i.e., <20 ps) found at 860–920 nm is similar to the rise of the PIA at 1250 nm. The nearly identical values found in the decay probed at ~900 nm and the rise probed at 1250 nm implies the evolution from a short-lived charge-transferred state to a long-lived charge transferred (mobile carrier) state, as in the diagram shown in Scheme 2. Fitting the data to an exponential decay yields a transition time of 15–17 ps for the 1:1 composite (both before and after annealing) and 7 ps for the annealed 1:3.3 composite.

The data obtained from the charge transfer band at 1250 nm in all bulk heterojunction composites indicate slow charge recombination; the PIA response remains almost constant in the nanosecond time regime. Measurements of the steady-state PIA probed in the near IR indicate that the photogenerated carriers live at least into the millisecond regime.[22] This slow charge recombination (reversed charge transfer to the ground state) is important for achieving high solar cell efficiency since it enables maximum collection of the photo-generated charges at the electrodes.

For high efficiency, however, the faster recombination of the initial charge-transferred state probed in the 900 nm PIA band (see Fig. 2) is a limiting factor. This relatively fast decay

indicates a loss of potentially useful photocarriers at times t < 600 ps from the intermediate charge transferred state shown in Scheme 2. Similar fast recombination components have been observed in poly(*p*-phenylene vinylene)s:C_{60}[13] and poly(thiophene)s:C_{60}.[16] Measurements at various light intensities indicate that bi-molecular carrier recombination is not important at the light intensity (40–200 μJ cm^{-2}) used for generating the data presented in Figures 2 and 4. Although not fully understood (perhaps a bound state between the electron on the PCBM and the hole on a nearby PCPDTBT chain) the elimination of this fast recombination channel is of paramount importance since long carrier lifetime is essential for improving the solar cell efficiency.

Figure 2 demonstrates that in annealed 1:3.3 material, the intermediate charge transferred state with PIA band at 900 nm (see Scheme 2) is almost completely eliminated compared to the long-lived PIA band (at 1200 nm) that arises from the mobile positive and negative carriers. Moreover, the annealed 1:3.3 material shows the fastest generation of long-lived mobile carriers. These observations are consistent with the enhanced solar cell efficiency obtained from annealed 1:3.3 composite compared to that of the 1:1 composites (both before and after annealing): Solar cells made with the annealed 1:3.3 composite yield efficiencies of 3.6 % while cells made from the 1:1 composites exhibit an efficiency of only ~1 %.[23] In the 1:3.3 material, therefore, the photo-generated carriers have lifetimes sufficient to enable higher collection efficiency.

In summary, ultrafast (t < 200 fs) charge separation was demonstrated for the PCPDTBT:PCBM materials. As shown in Scheme 2, the relaxation dynamics in this small band gap polymer bulk heterojunction material suggest a two step charge transfer process: The PIA from an intermediate charge transferred state (perhaps a bound state with the electron on the PCBM and the hole on the nearby PCPDTBT) converts into the PIA from the long-lived mobile carriers on their respective phase separated networks. If carrier recombination to the ground state occurs from the intermediate state, the corresponding fraction of mobile carriers is lost and does not contribute to the macroscopic photocurrent. The optimal system for solar cell applications is the annealed 1:3.3 PCPDTBT:PCBM composite which exhibits the smallest contribution from the intermediate charge transferred state and the largest contribution from the long-lived mobile carriers. Cells made from the annealed 1:3.3 PCPDTBT:PCBM composite exhibit correspondingly higher power conversion efficiencies. Since the relatively short-lived charge transferred state limits the efficiency of polymer-based solar cells, further optimization of the microstructure and morphology of the PCPDTBT:PCBM bulk heterojunction material might be possible.

Experimental

The synthesis of the small band gap polymer PCPDTBT will be described elsewhere [22]. The photovoltaic applications of the PCPDTBT were published [23]. The samples used in the measurements were prepared in a nitrogen glove-box with an oxygen concentration of ~1.5 ppm. In order to study the electron transfer dynamics in the high concentration regime relevant to photovoltaic cells, 1:1 and 1:3.3 PCPDTBT:PCBM composites containing 50 and 77 % by weight PCBM, respectively, were prepared. In these studies we used the C_{60} derivative, PCBM, provided by Konarka Technologies.

All films (both pristine PCPDTBT and PCPDTBT:PCBM composites) were spin-cast at 1000 rpm from ortho-dichlorobenzene solution (10 mg mL^{-1}) onto quartz substrates. The optical densities were ~1.0 at the maximum absorption energy. Following spin-casting, the films were dried at room temperature or annealed for 10 minutes at 120 °C. Samples were kept under dynamic vacuum (< 10^{-4} mbar) during all TA measurements.

The absorption spectra were recorded by using a spectrometer (Shimadzu UV-2401 PC). The photoluminescence spectra were obtained using a fluorimeter (Photon Technology International) equipped with a Xenon lamp as the light source; the samples were excited by monochromatic light (λ ~ 750 nm) at an incidence angle of ~45°, and the emitted radiation was collected at ~45°, dispersed by a monochromator, and recorded by a liquid nitrogen cooled germanium detector (Edinburgh Instruments).

The TA measurements were carried out with a dual-beam femtosecond spectrometer utilizing the second harmonic of an OPA (optical parametric amplifier) as the pump and a white light continuum as the probe [12]. The TA spectra of pristine PCPDTBT were measured at several delay times at each probe wavelength using constant pump fluence. The TA spectra of PCPDTBT:PCBM composites were recorded by a scanning monochromator in the 380–1500 nm spectral region. Group velocity dispersion in the probe was compensated by shifting the delay in order to keep the pump-probe delay time fixed at each wavelength. The error in the spectral region at λ > 1200 nm is greater than at shorter wavelengths because of the weak probe beam generated at this region. A germanium detector was used for detecting the TA signals in the near IR regime.

At each probe energy, the TA decay time constants were obtained by de-convoluting the measured signal from the pump Gaussian time-profile, characterized by a full width at half maximum of ~200 fs. The resulting decay profile was then fitted to a sum of exponential terms.

Received: October 27, 2006
Revised: February 2, 2007
Published online: July 24, 2007

[1] W. Ma, C. Yang, X. Gong, K. Lee, A. J. Heeger, *Adv. Funct. Mater.* **2005**, *15*, 1617.
[2] J. Y. Kim, S. H. Kim, H.-H. Lee, K. Lee, W. Ma, X. Gong, A. J. Heeger, *Adv. Mater.* **2006**, *18*, 572.
[3] C. Winder, N. S. Sariciftci, *J. Mater. Chem.* **2004**, *14*, 1077.
[4] M. R. Andersson, O. Thomas, W. Mammo, M. Svensson, M. Theander, O. Inganäs, *J. Mater. Chem.* **1999**, *9*, 1933.
[5] A. Dhanabalan, J. K. J. van Duren, P. A. van Hal, J. L. J. van Dongen, R. A. J. Janssen, *Adv. Funct. Mater.* **2001**, *11*, 255.
[6] C. J. Brabec, C. Winder, N. S. Sariciftci, J. C. Hummelen, A. Dhanabalan, P. A. van Hal, R. A. J. Janssen, *Adv. Funct. Mater.* **2002**, *12*, 709.
[7] C. Winder, G. Matt, J. C. Hummelen, R. A. J. Janssen, N. S. Sariciftci, C. J. Brabec, *Thin Solid Films* **2002**, *403–404*, 373.
[8] M. Svensson, F. Zhang, S. Veenstra, W. J. H. Verhees, J. C. Hummelen, J. M. Kroon, O. Inganäs, M. R. Andersson, *Adv. Mater.* **2003**, *15*, 988.
[9] X. Wang, E. Perzon, F. Oswald, F. Langa, S. Admassie, M. R. Andersson, O. Inganäs, *Adv. Funct. Mater.* **2005**, *15*, 1665.
[10] H. Aarnio, M. Westerling, R. Österbacka, M. Svensson, M. R. Andersson, T. Pascher, J. Pan, V. Sundström, H. Stubb, *Synth. Met.* **2005**, *155*, 299.
[11] N. S. Sariciftci, L. Smilowitz, A. J. Heeger, F. Wudl, *Science* **1992**, *258*, 1474.

[12] B. Kraabel, D. McBranch, N. S. Sariciftci, D. Moses, A. J. Heeger, *Phys. Rev. B* **1994**, *50*, 18 543.
[13] B. Kraabel, J. C. Hummelen, D. Vacar, D. Moses, N. S. Sariciftci, A. J. Heeger, *J. Chem. Phys.* **1996**, *104*, 4267.
[14] C. J. Brabec, G. Zerza, G. Cerullo, S. D. Silvestri, S. Luzzati, J. C. Hummelen, S. Sariciftci, *Chem. Phys. Lett.* **2001**, *340*, 232.
[15] J. G. Müller, J. M. Lupton, J. Feldmann, U. Lemmer, M. C. Scharber, N. S. Sariciftci, C. J. Brabec, U. Scherf, *Phys. Rev. B* **2005**, *72*, 195 208.
[16] B. Kraabel, C. H. Lee, D. McBranch, D. Moses, N. S. Sariciftci, A. J. Heeger, *Chem. Phys. Lett.* **1993**, *213*, 389.
[17] P. A. van Hal, R. A. J. Janssen, G. Lanzani, G. Cerullo, M. Zavelani-Rossi, S. D. Silvestri, *Chem. Phys. Lett.* **2001**, *345*, 33.
[18] R. Österbacka, C. P. An, X. M. Jiang, Z. V. Vardeny, *Science* **2000**, *287*, 839.
[19] C. Soci, I.-W. Hwang, D. Moses, Z. Zhu, D. Waller, R. Gaudiana, C. J. Brabec, A. J. Heeger, *Adv. Funct. Mater.* **2007**, *17*, 632.
[20] X. Jiang, R. Österbacka, O. Korovyanko, C. P. An, B. Horovitz, R. A. J. Janssen, Z. V. Vardeny, *Adv. Funct. Mater.* **2002**, *12*, 587.
[21] S. V. Frolov, M. Liess, P. A. Lane, W. Gellermann, Z. V. Vardeny, M. Ozaki, K. Yoshino, *Phys. Rev. Lett.* **1997**, *78*, 4285.
[22] Z. Zhu, D. Waller, R. Gaudiana, D. Mühlbacher, M. Morana, M. C. Scharber, C. Brabec, *Macromolecules* **2007**, *40*, 1981.
[23] D. Mühlbacher, M. Scharber, M. Morana, Z. Zhu, D. Waller, R. Gaudiana, C. Brabec, *Adv. Mater.* **2006**, *18*, 2884.

